Comparative study of the collisional electron detachment of C^-, Si^-, and Ge^- by light noble gases

H. Luna, F. Zappa, M. H. P. Martins, S. D. Magalhães, Ginette Jalbert, L. F. S. Coelho, and N. V. de Castro Faria
Instituto de Física, Universidade Federal do Rio de Janeiro, Caixa Postal 68528, Rio de Janeiro, 21945-970, RJ, Brazil
(Received 10 November 2000; published 17 April 2001)

Collisional electron detachment of anions with np^3 structures ($n=2, 3$, and 4), namely, C^-, Si^-, and Ge^-, was studied for He, Ne, and Ar targets and relative velocities ranging from 0.2 a.u. to 2.2 a.u.. Single, double, and triple electron ejection cross sections were also measured for the C^- anion colliding with an Ar target, being observed to obey a binomial distribution. Two striking universal features were observed concerning the total detachment cross sections: for each target a multiplicative scaling may be made for the cross sections of the three projectiles, and these factors are target independent. The maxima of these three curves show a nonmonotonic correspondence with the noble-gas atomic numbers. A simple law, proposed for the scaling, indicates the presence of metastable states in the Si^- and Ge^- beams.

DOI: 10.1103/PhysRevA.63.052716 PACS number(s): 34.50.Fa, 34.90.+q

I. INTRODUCTION

Studies of the group-IV semiconductor elements, such as carbon, silicon, and germanium, are of interest to microelectronics and materials science. Concerning their clusters, carbon buckyballs have been the object of thousands of works, and phenomena involving small silicon [1] and germanium [2] cluster anions have also recently been studied. In particular, theoretical calculations of cluster structures and growth patterns, as the number of atoms increase, have also been reported [3]. Nevertheless relatively few works are concerned with collisions involving atomic and small carbon, silicon and germanium cluster anions [4], pointing to the need of such investigations.

Recently [5], we reported the measurement of Si^- electron detachment cross sections on He, Ne, and Ar targets, in the relative velocity range 0.25–1.4 a.u., the most surprising feature of these data being their strong resemblance with the H^- detachment results for the same target gases [6,7]. The Si^- cross sections present a maximum for each target gas at almost the same velocities as in the H^- case (which are 0.44 a.u. for He, 1.30 a.u. for Ne, and 1.06 a.u. for Ar), showing the same nonmonotonic correspondence with the target atomic number. For any given target the overall shapes of the two cross-section curves were similar, allowing the use of very simple additive and multiplicative scalings. This similarity among the two projectiles, Si^- and H^-, even extended to both presenting the tendency for He and Ne data to intersect each other at the lowest measured velocities [6,7].

The velocity range in our previous paper [5] covers the transition from low to high velocity regimes, where different mechanisms operate. In the high velocity regime, we can make a simplified description of the collision process as the scattering of the assumed free projectile electron(s) by the target, with detachment occurring when the energy transfer, as measured in the projectile nucleus rest frame, exceeds the binding energy of the electron(s). Two expected features of the cross sections, actually observed, were their increase with the atomic number of the target for a given velocity, and their decrease with the relative velocity for a given target atom.

In the low-velocity regime a quasi molecular picture is used to interpret the Si^- case, albeit only qualitatively because the anionic SiHe and SiNe structures have not yet been calculated. In the H^- case, however, calculations have been performed and indicate transitions among AH^- and AH intersecting quasimolecular states, where A represents He or Ne [8]. For Ne the distinct behavior of the two potential-energy curves can be interpreted as an inhibition of the H^- electron detachment, lowering the low-velocity cross sections (quasimolecular regime) and displacing the maximum to a higher-velocity position, thus explaining the almost flat results observed.

Another interesting feature was that all our measured Si^- electron detachment cross sections were higher than for H^-. It is known that Si^- has three electrons in the $3p^3$ sub-shell, and predicted excited long-lived ^2D and ^2P terms [9–11] (Table I). However, due to their different configurations, comparison of the Si^- and H^- detachment results was not sufficient to confirm the existence of metastable states in the Si^- beam.

The collisional detachment cross sections of H^- and the alkali-metal anions, Li^-, Na^-, and K^- are known to satisfy simple multiplicative scalings [12], understandable in terms of their common ns^2 configurations. A similar reasoning, however, does not apply to the scaling of the Si^- and H^- detachment data, thereby suggesting the importance of a more extensive study of detachment in group-IV anions.

Carbon and germanium anions, like silicon, have three electrons in the p subshell. The ^2D state of carbon has a very small electron affinity [9] and the existence of an excited

TABLE I. Binding energies of ground and metastable states of C^-, Si^-, and Ge^-.

Anion	Binding energies (eV) (Anderson *et al.* [11]) S	D	P
C^-	1.2621	0.033	
Si^-	1.3895	0.5272	0.029
Ge^-	1.2327	0.4014	

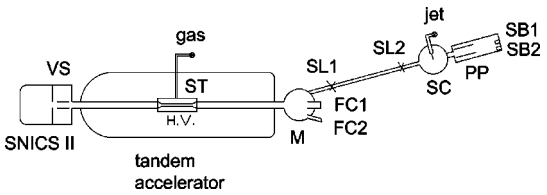

FIG. 1. Experimental setup. Shown are the sputtering ion source (SNICS-II), magnet (M), velocity selector (VS), stripper gas cell (ST), and Faraday cups (FC1 and FC2) used in measurements of total-electron cross sections. In the 15° beam line are shown the slits (SL1 and SL2), the scattering chamber (SC), and the detection system composed by a set of two charged parallel plates (PP) and two surface-barrier detectors (SB1 and SB2).

Ge^- (^2D) term has been reported in the literature [13]. All relevant affinities are listed in Table I. A comparison of electron detachment cross sections of Si^- and Ge^- with those of C^- may be used to check the existence of metastable states in the beam; in fact, for the electron detachment of alkali-metal anions in noble gases, at intermediate and high velocities, Andersen and co-workers [12] obtained multiplicative factors that roughly scaled with the inverse square of the binding energy. Should some similar monotonic rule work for semiconductor anions, we would have a good probe for the presence of metastable states.

In this work some results of such a systematic study of the collisional electron detachment of C^-, Si^-, and Ge^- anions, are reported. The total detachment cross sections have been measured for He, Ne, and Ar targets. Considering that results obtained in our previous work (for one velocity and target) [5] on the ejection of one, two, and three electrons seemed to indicate that the electrons were independently ejected [14], a systematic study has also been made of the single- and multiple-electron ejection for the C^- anion colliding with an Ar target.

II. EXPERIMENT

The experiments were performed at the Laboratório de Colisões Atômicas e Moleculares (LaCAM) of the Universidade Federal do Rio de Janeiro (UFRJ). The experimental setup is shown in Fig. 1. Beams of C^-, Si^-, and Ge^- were produced by a cesium vapor sputtering ion source (SNICS-II). The ions were preaccelerated to a kinetic energy E_p and, after mass selection in a Wien filter, acquire an additional energy $e\times V$ in the first stage of our laboratory's 5SDH Pelletron accelerator, in which the potential V may be as high as 1.7 MV. With that energy ($E_p+e\times V$), they go through the gas stripper.

All our measurements of total electron detachment cross sections were made using the stripper gas as target, as described in Refs. [5,15]. This method is feasible because the pressure of the gas, which is introduced from outside through a pressurized insulating tube and regulated by an externally controllable valve, though not directly measurable, is nevertheless known. For each gas (He, Ne, and Ar), published values of single-electron-loss cross sections of H^- were used to make a correspondence between the stripper gas pressure and the readings of an ion gauge, placed at the grounded high-energy end of the accelerator.

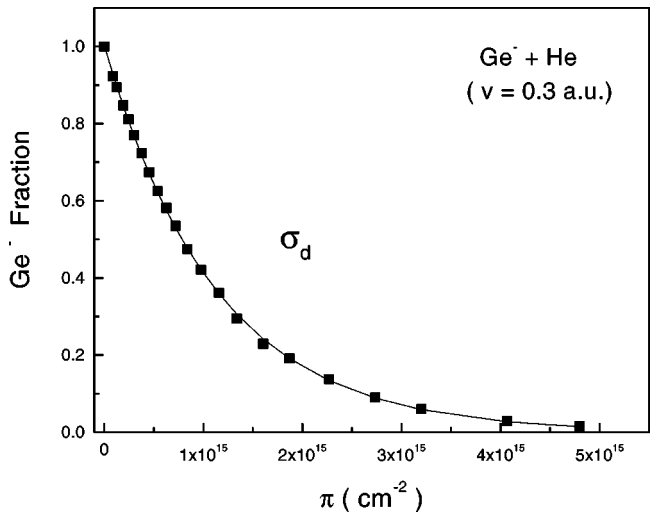

FIG. 2. Typical exponential decay curve used to obtain total-electron detachment cross sections, obtained by varying the target thickness and measuring the final anion current in Faraday cup 2 (FC2).

The total (and absolute) detachment cross sections were extracted from exponential decay curves, obtained by varying the target pressure [5,15,16], as shown in a typical case in Fig. 2. Normalization was simple due to the stability of the accelerator beam current for time intervals of a few minutes. Uncertainties in the exponential fitting procedure and in the cross-section values used in the stripper pressure calibration are the main causes of uncertainty in the measured cross sections, estimated to be around 4% to 7%.

A second set of experiments, namely, the detachment of one, two, and three electrons of C^- at different velocities has also been performed, but now using a gas target placed inside the scattering chamber (shown in Fig. 1) and a C^- beam obtained through an indirect process. Sputtering in the ion source may produce both C^- and C_2^- beams which in the stripper may give origin, among other possibilities, to C and C_2^+ ions, respectively. Collisions of those ions with the residual gas, in the region between the high-energy end and the switching magnet (M), provide final C^- beams with the same energy/mass ratio (and thus indistinguishable under magnetic selection): the former by capture of one electron and the latter by fragmentation.

The resulting C^- beam, after being momentum analyzed in the switching magnet and deflected to 15°, is collimated to a diameter of less than 0.4 mm by micrometric sliding slits; this drastic collimation reduces the beam intensity to values that were kept smaller than 300 particles per second. With such counting rates, surface-barrier detectors could be employed, as indicated in Fig. 1, ensuring a continuous check of the beam energy and composition, and giving the advantage of 100% efficiency.

The highly collimated beam hits the gas target, a gaseous jet provided by a hypodermic needle. With no jet, the vacuum in the scattering chamber was better than 10^{-7} Torr, being 10^{-8} Torr at the high-energy end of the accelerator.

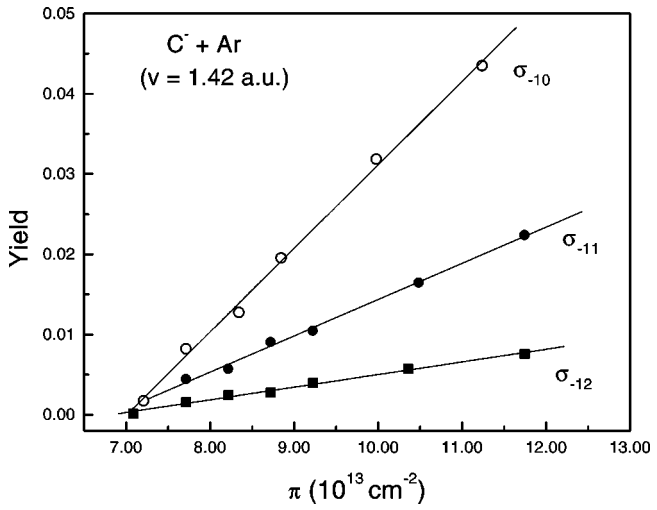

FIG. 3. Typical growth curves used to obtain the cross sections σ_{10}^{-}, σ_{11}^{-}, and σ_{12}^{-}. In these measurements the final-state beam was measured by the two surface-barrier detectors, SB1 and SB2.

The target thickness was obtained from the pressure readings in the chamber, through a calibration process using published $H^- \rightarrow H$ single-electron detachment cross-section values [16]. Ions, in charge states one or two, were deflected to the surface-barrier detector SB2 by conveniently setting the electric field of parallel electrostatic plates (PP), placed just after the target; neutral particles were measured with SB1. The incident beam was also measured, with SB2 or SB1 (with no electric field applied). The growth rate method was used to extract the cross sections [16], as shown in a typical case in Fig. 3.

III. RESULTS AND DISCUSSION

Figure 4(a) shows the absolute electron detachment cross sections of C^-, Si^- and Ge^- anions in Ar. In Fig. 4(b) the Si^- and Ge^- results were scaled to the C^- results, taken as reference, through multiplicative factors K shown in Table II. In all cases there is a striking similarity of results, in particular the maxima are in excellent agreement with each other. Finally, the measured detachment cross sections of one, two, and three electrons of C^- anions in Ar are shown in Table III. These results, after being normalized to their sum for each velocity, i.e., $F(v)=\sigma_{1i}^{-}(v)/\Sigma_i \sigma_{1i}^{-}$, are also shown in Fig. 5.

The good agreement of the Si^-,Ge^-, and C^- curves for collisions with He, Ne, and Ar, shown in Fig. 4(b), particularly at high velocities, is not fortuitous and point to a very simple scaling for these three-*p*-electrons systems. As shown in Table II, within the experimental fluctuations there is essentially a single average *K* factor, $\langle K \rangle$, for Si^- and another for Ge^-, irrespective of the target atom, although a very small *Z* dependence may hold.

To understand these remarkable features, we tried at first to apply the simple scaling that Andersen *et al.* [12] have employed for anions with ns^2 structures, namely H^-, Li^-, Na^-, and K^- incident on He, Ne, and Ar, observing that the multiplicative factors are proportional to the inverse of the

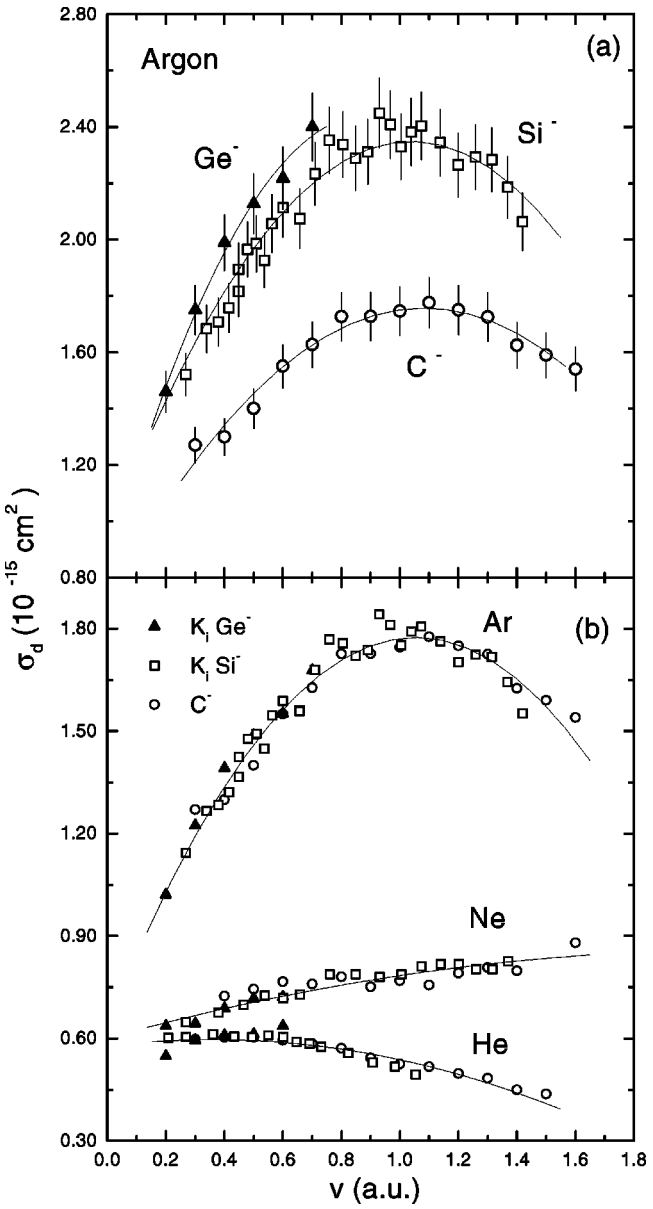

FIG. 4. (a) Absolute electron detachment cross sections of C^- (circle), Si^- (square) [5], and Ge^- (triangle) incident on Ar. (b) Electron detachment cross sections of C^- (circle) incident on He, Ne, and Ar compared with the results for Si^- (square) and Ge^- (triangle) scaled by the multiplicative factors $\langle K \rangle$ of Table II. The solid lines are drawn only to guide the eye.

squared electron affinities [12]. In our case it has the form

$$\frac{\sigma_i}{\sigma_{C^-}} = \left(\frac{n_g(i)}{I_g^2(i)} + \frac{n^*(i)}{I^{*2}(i)} \right) I_g^2(C), \tag{1}$$

where the index *i* stands for silicon or germanium and the carbon anion is assumed to be in the ground state. The (I_g, I^*) are the electron affinities given in Table I for the ground and metastable states, respectively, and (n_g, n^*) their populations. The (σ_i, σ_{C^-}) are the detachment cross sections of silicon or germanium and carbon, respectively. For the populations of metastable and ground states,

TABLE II. Multiplicative factors that scale to each other the detachment cross sections of C^-,Si^-, and Ge^- as shown in Fig. 4(b). $\langle K \rangle$ is the average K for each anion.

	K			
Anions	He	Ne	Ar	$\langle K \rangle$
C^-	1.00	1.00	1.00	1.00
Si^-	0.78	0.76	0.75	0.76
Ge^-	0.67	0.70	0.70	0.69

$$n_g(i) + n^*(i) = 1. \tag{2}$$

Some assumptions were made for solving Eqs. (1) and (2). First, any influence of the D state of C^- or the P state of Si^- was neglected. In fact, as stated by Nadeau and Litherland [17], the population of weakly (some meV) bound metastable states is usually destroyed by high electric fields produced by irregularities on the sputtered target surface. Second, the scaling law proposed by Andersen *et al.* [12] was assumed valid in the intermediate velocities range. With these assumptions metastable Si^- and Ge^- fractions, around 10% and 5%, respectively, and the remaining anions in the ground state, were obtained. Balling *et al.* [18], using a different kind of sputtering ion source, obtained less than 2% of the Si^- beam in the metastable ^2D state. Scheer *et al.* [9] have also observed metastable anions via infrared laser spectroscopy measurements, though in the 0.1% scale.

Two possibilities for the disagreement between the present estimates of the metastable fractions and the experimental values of references [9,18] are suggested. First, the scaling model, verified to work at high velocities and for alkali-metal anions, has been applied in the intermediate velocities range and for group-IV elements, where it may not work so well. Second, the metastable component could be very sensitive to the sputtering ion source and operation conditions. Considering the effective temperature equal to the room temperature, the metastable fractions obtained using the Boltzmann factor would be smaller than 1%, both for silicon and germanium. On the other hand, Norskov *et al.* [19] have estimated a nonequilibrium effective temperature of 9000 K for a typical Cu^+ ion beam obtained by sputtering. In our case, the metastable populations for the silicon and germanium anions obtained from the scaling model indicate an effective temperature around 5000 K.

TABLE III. Measured single, double, and triple electron detachment cross sections for C^- incident on Ar for velocities in the interval 1.0–2.2 a.u.

	$\sigma\ (10^{-15}\ \text{cm}^2)$		
v (a.u.)	σ_{10}^-	σ_{11}^-	σ_{12}^-
1.00	1.19±0.14	0.45±0.05	0.12±0.01
1.16	1.13±0.14	0.46±0.06	0.13±0.02
1.30	1.14±0.14	0.46±0.06	0.14±0.02
1.42	1.04±0.13	0.45±0.05	0.16±0.02
1.60	0.96±0.12	0.45±0.05	0.20±0.02
1.84	0.90±0.11	0.43±0.05	0.18±0.02
2.05	0.75±0.09	0.38±0.05	0.18±0.02
2.20	0.70±0.08	0.34±0.04	0.14±0.02

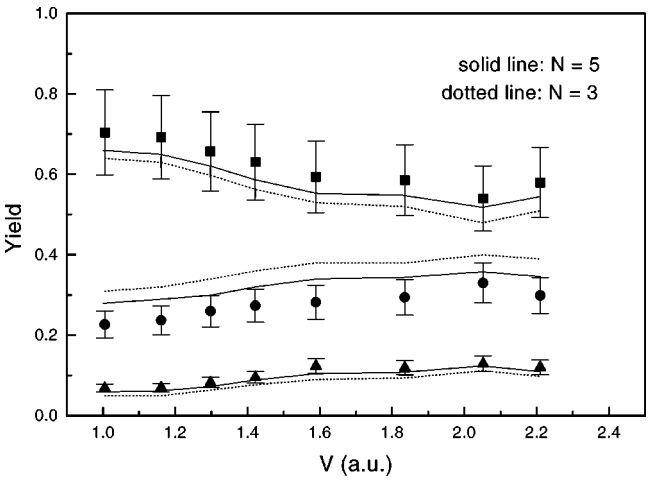

FIG. 5. Fractional relative detachment cross sections of one (solid square), two (solid circle), and three (solid triangle) electrons of C^- in collision with Ar, normalized to one for each measured velocity. Also shown as a dotted line ($N=3$) and a solid line ($N=5$) are the normalized probabilities P_n^N of a binomial distribution that best fits the experimental results, at each velocity.

In order to understand the general shapes of the cross sections, particularly the nonmonotonic variation in the positions of the maxima corresponding to He, Ne, and Ar, we should first understand how the maxima are formed. As already stated, we interpreted these maxima as a consequence of a transition from the low- to the high-velocity collisional regimes, where different physical processes occur. The high-velocity region does not present special features and the detachment of electrons is essentially a geometric effect: the highest cross section for argon, the lowest for helium. However, in the low-velocity region the structure of both collisional partners plays an important role, as already pointed out by Olson and Liu [8] in the case of H^-. As the maxima corresponding to He and Ar are at predictable relative positions, an explanation for the almost flat curve of Ne, with its maximum dislocated to a high velocity, should be searched in a comparison of the Ne and He curves at low velocities.

In fact when an anion A^- collides with an atom X at low relative velocities, its electrons can be removed by a transition between the molecular states AX^- and AX, if they intersect. These states have been calculated [8] for the anion H^- colliding with He or Ne, considering the molecular states HeH^- and HeH (or NeH^- and NeH). For helium, the curves intersect at a distance R_c of the order of $2.7a_0$. For a sufficiently close approach of H^- and He, such that their internuclear separation R is less than $2.7a_0$, the system can cross to the HeH state, ejecting the attached electron.

For H^- colliding with Ne, however, the situation is somewhat different. The NeH^- and NeH states do not intersect but merge, for R lower than approximately $1.9a_0$, which results in a detachment cross section smaller by a factor of about 2/3, as compared to that of H^- colliding with He. That

is why the cross sections for H^- colliding with He and Ne intersect at $v \simeq 0.77$ a.u.: the inhibition of the cross section for Ne makes its maximum flat and far from those of He and Ar. The same inhibition has only a secondary effect on argon.

The single-, double-, and triple-electron detachment cross sections of carbon, listed in Table III, may be analyzed employing simple binomial distributions of single-electron probabilities [14]. For such an analysis, in a first step, the measured detachment cross sections at a given velocity (single, double, and triple) were normalized by dividing them by their sum. The resulting fractions, for C^- colliding with Ar, are shown as solid symbols in Fig. 5. In a second step, the binomial probabilities $P_n^N = \binom{N}{n} p^n (1-p)^{N-n}$ (with $n=1$, single detachment; $n=2$, double; $n=3$, triple) were also divided by their sum and, for each velocity, the value of p that best fitted all three normalized cross sections was found. The dotted line in Fig. 5 connects the resulting normalized binomial probabilities, calculated with $N=3$ (number of available electrons in the p^3 subshell) and the solid line those for $N=5$ (number of available electrons in the most external shell). Though not excellent, the agreement attained suggests independent electron detachment, perhaps with a slight contribution of the two extra electrons that do not belong to the np^3 structure.

Such simple binomial distributions of single-electron probabilities have been employed by other authors to describe the multiple inner-shell ionization in fast collisions, where the effects of both the electron correlation and the electron exchange are expected to be small [20]. This approach has also been used for multiple ionization in outer shells, where electron correlation is not expected to be so small [21]. As the validity of the binomial distribution rests on the neglect of electron correlation in both initial and final states, we can assume that the detachment of the three outer electrons of C^-, in the intermediate-velocity regime, is essentially event independent and, as the ejection of these electrons accounts for almost the total electron detachment cross sections, calculations based on the independent scattering model would be appropriate [22]. Andersen *et al.* [12] have arrived at similar conclusions, after analyzing the $Li^- + He$ collision at low velocities; they estimated the correlation effect and pointed out that it has little influence on the total electron detachment [12,23].

IV. CONCLUSIONS

Our analysis of the total electron detachment cross sections of C^-, Si^-, and Ge^- colliding with He, Ne, and Ar has shown that they all share a common shape in their dependence with the relative collisional velocity. Single multiplicative factors were found, one for Si^- and another for Ge^-, which scale their cross sections to those of C^-, for all targets. A simple scaling law was then applied, strongly suggesting the presence of metastable Ge^- and Si^- ions. The observed inversion in the position of the cross-section maxima for the He and Ne targets has also been qualitatively understood on the basis of a quasimolecular description.

As a final conclusion, detachment cross sections of one, two, and three electrons of carbon, expressed as fractions of their sum at each relative collisional velocity, were compatible with a binomial distribution. Such independence of the electron detachment cross sections on the multiple ionization of charged projectiles opens the possibility of extending the free-collision classical impulse approximation to the screening contribution of electron-loss calculations [24].

ACKNOWLEDGMENTS

This work was partially supported by the Brazilian agencies CNPq, FAPERJ, and FUJB.

[1] S. Li, R.J. Van Zee, W. Weltner, Jr., and K. Raghavachari, Chem. Phys. Lett. **243**, 275 (1995).
[2] G.R. Burton, C. Xu, C.C. Arnold, and D.M. Neumark, J. Chem. Phys. **104**, 2757 (1996).
[3] A.A. Shvartsburg, B. Liu, Z.Y. Lu, C.Z. Wang, M.F. Jarrold, and K.M. Ho, Phys. Rev. Lett. **83**, 2167 (1999).
[4] H.B. Pedersen, N. Djuric, M.J. Jensen, D. Kella, C.P. Safvan, H.T. Schmidt, L. Vejby-Christensen, and L.H. Andersen, Phys. Rev. A **60**, 2882 (1999).
[5] H. Luna, S.D. Magalhães, J.C. Acquadro, M.H.P. Martins, W.M.S. Santos, Ginette Jalbert, L.F.S. Coelho, and N.V. de Castro Faria, Phys. Rev. A **63**, 022705 (2001).
[6] M. Meron and B.M. Johnson, Phys. Rev. A **41**, 1365 (1990).
[7] Y. Nakai, T. Shirai, T. Tabata, and R. Ito, At. Data Nucl. Data Tables **37**, 69 (1987).
[8] R.E. Olson and B. Liu, Phys. Rev. A **22**, 1389 (1980).
[9] M. Scheer, R.C. Bilodeau, C.A. Brodie, and H.K. Haugen, Phys. Rev. A **58**, 2844 (1998).
[10] J. Thogersen, L.D. Steele, M. Scheer, C.A. Brodie, and H.K. Haugen, J. Phys. B **29**, 1323 (1996).
[11] H. Hotop and W.C. Lineberger, J. Phys. Chem. Ref. Data **14**, 731 (1985); T. Andersen, H.K. Haugen, and H. Hotop, *ibid.* **28**, 1511 (1999).
[12] N. Andersen, T. Andersen, L. Jepsen, and J. Macek, J. Phys. B **17**, 2281 (1984).
[13] D. Feldman, R. Rackwitz, E. Heinicke, and H.J. Kaiser, Z. Naturforsch. A **32**, 302 (1997).
[14] J.H. McGuire, *Electron Correlation Dynamics in Atomic Collisions* (Cambridge University Press, Cambridge, 1997).
[15] J.C. Acquadro, H. Luna, S.D. Magalhães, F. Zappa, Ginette Jalbert, E. Bessa Filho, L.F.S. Coelho, and N.V. de Castro Faria, Nucl. Instrum. Methods Phys. Res. B **172**, 82 (2000).
[16] D.P. Almeida, N.V. de Castro Faria, F.L. Freire, Jr., E.C. Montenegro, and A.G. de Pinho, Phys. Rev. A **36**, 16 (1987).
[17] M-J. Nadeau and A.E. Litherland, Nucl. Instrum. Methods Phys. Res. B **52**, 387 (1990).
[18] P. Balling, P. Kristensen, H. Stapelfeldt, T. Andersen, and H.K. Haugen, J. Phys. B **26**, 3531 (1993).
[19] J.K. Norskov and B.I. Lundqvist, Phys. Rev. B **19**, 5661 (1979).

[20] R.L. Kauffman, J.H. McGuire, P. Richard, and C.F. Moore, Phys. Rev. A **8**, 1233 (1973).
[21] M.B. Shah, C.J. Patton, J. Geddes, and H.G. Gilbody, Nucl. Instrum. Methods Phys. Res. B **98**, 280 (1995).
[22] Vu Ngoc Tuan and J.P. Gauyacq, J. Phys. B **20**, 3843 (1987).
[23] T. Andersen and J. Engholm Pedersen, J. Phys. B **22**, 617 (1993).
[24] W.S. Melo, M.M. SantAnna, A.C.F. Santos, G.M. Sigaud, and E.C. Montenegro, Phys. Rev. A **60**, 1124 (1999).